Bergmann, I., Dobslaw, H. (2012): Short-term transport variability of the Antarctic circumpolar current from satellite gravity observations. - Journal of Geophysical Research, 117, C05044

DOI: 10.1029/2012JC007872

Short-term transport variability of the Antarctic Circumpolar Current from satellite gravity observations

I. Bergmann[1] and H. Dobslaw[1]

Received 2 January 2012; revised 23 March 2012; accepted 9 April 2012; published 30 May 2012.

[1] Ocean bottom pressure gradients deduced from the satellite gravity mission Gravity Recovery and Climate Experiment (GRACE) were previously shown to provide barotropic transport variations of the Antarctic Circumpolar Current (ACC) with up to monthly resolution. Here, bottom pressure distributions from GRACE with monthly (GFZ RL04) and higher temporal resolution (CNES/GRGS with 10 days, ITG-GRACE2010 with daily resolution) are evaluated over the ACC area. Even on time scales shorter than 10 days, correlations with in situ bottom pressure records frequently exceed 0.6 with positive explained variances, giving evidence that high-frequency nontidal ocean mass variability is captured by the daily ITG-GRACE2010 solutions not already included in the applied background models. Bottom pressure is subsequently taken to calculate the barotropic component of the ACC transport variability across Drake Passage. For periods longer than 30 days, transport shows high correlations between 0.4 and 0.5 with several tide gauge records along the coast of Antarctica. Still significant correlations around 0.25 are obtained even for variability with periods shorter than 10 days. Since transport variations are predominantly affected by time-variable surface winds, GRACE-based transports are contrasted against an atmospheric index of the Southern Annular Mode (SAM), which represents the Southern Hemispheric wind variability. Correlations between the SAM and GRACE-based transports are consistently higher than correlations between any of the available sea level records in all frequency bands considered, indicating that GRACE is indeed able to accurately observe a hemispherically consistent pattern of bottom pressure (and hence ACC transport) variability that is otherwise at least partially masked in tide gauge records due to local weather effects, sea ice presence and steric signals.

Citation: Bergmann, I., and H. Dobslaw (2012), Short-term transport variability of the Antarctic Circumpolar Current from satellite gravity observations, *J. Geophys. Res.*, *117*, C05044, doi:10.1029/2012JC007872.

1. Introduction

[2] Strong westerly winds and the absence of land barriers in the middle latitudes of the Southern Hemisphere allow for the establishment of the Antarctic Circumpolar Current (ACC). Being the dominant feature of global ocean dynamics in terms of transport, it carries in average 136 ± 11 Sv [*Cunningham et al.*, 2003] through Drake Passage into the South Atlantic. By connecting all major ocean basins, the ACC permits the existence of a global overturning circulation allowing for the global exchange of freshwater, heat, nutrients, and other oceanic tracers that affect the evolution of the climate on our planet.

[3] While the time mean ACC transport is related to the interplay of various dynamic processes including topographic and eddy-induced stresses as well as stratification (see, e.g., *Rintoul et al.* [2001] and *Olbers et al.* [2004] for a review), fluctuations in the southern hemispheric wind field are primarily responsible for variations of the transport in time. Based on theoretical argumentation and numerical experiments, *Hughes et al.* [1999] explain that topographically modified barotropic Rossby waves, resonantly excited by the varying winds, mediate the response along f/H contours passing through the Drake Passage and encircling the continent, and lead to coherent variations in meridional bottom pressure gradients all around Antarctica. For reasons of geostrophy, pressure changes are more pronounced along the southern rim of the current, implying that bottom pressure sensors and sea level gauges close to the Antarctic coast are suitable to monitor the barotropic component of the ACC transport variations [e.g., *Woodworth et al.*, 2006]. In addition, numerical model experiments by *Olbers and Lettmann* [2007] indicate that correlations between bottom pressure changes and ACC transport remain strong for synoptic and annual time scales, with baroclinic processes gradually

[1]Deutsches GeoForschungsZentrum, Potsdam, Germany.

Corresponding author: I. Bergmann, Deutsches GeoForschungsZentrum, Telegrafenberg A20, Potsdam D-14473, Germany. (inga.bergmann@gfz-potsdam.de)

0148-0227/12/2012JC007872

gaining importance on decadal periods and longer. Thus, measurements of bottom pressure gradients around Antarctica are a valuable observable to monitor the transient variations of ACC mass transports, particularly on time scales beyond a few years.

[4] The ACC is driven by the surface winds. Whether its forcing is dominated by the wind stress via an Ekman-type mechanism, or the wind stress curl by means of a time-variable Sverdrup-type vorticity balance still remains controversial [e.g., *Hughes et al.*, 1999; *Gille et al.*, 2001]. However, the ACC transports may be assumed to vary in response to changes in the Southern Annular Mode (SAM) [*Thompson and Wallace*, 2000]. This mode, excited internally within the midlatitude's troposphere, is characterized by zonally symmetric atmospheric mass shifts between polar and moderate latitudes and associated vacillations in the surface wind fields. The mode explains up to 30% of the deseasonalized variability in both geopotential and winds. Antarctic sea level variations, and thus ACC transport, were found to be correlated to the SAM down to seasonal time scales [*Meredith et al.*, 2004], although *Cunningham and Pavic* [2007] concluded that SAM-related modes cannot be detected in surface currents derived from repeated hydrographic sections and 12 years of satellite altimeter observations. Moreover, SAM variability can be characterized by a normally distributed red noise process with an *e*-folding time scale of 10 days, implying that substantial variability of the SAM is found even on a week-to-week basis, which might potentially be related to short-term variability present in both bottom pressure and current meter observations in the Southern Ocean [see, e.g., *Whitworth and Peterson*, 1985].

[5] By mapping temporal variations of the Earth's gravity field, the Gravity Recovery and Climate Experiment (GRACE) [*Tapley et al.*, 2004] satellite mission provides for the first time an opportunity to observe changes in the global ocean bottom pressure distribution covering synoptic to interannual time scales. Seasonal variations in regional bottom pressure from GRACE have been shown to be consistent with prevailing winds in the North Pacific [*Bingham and Hughes*, 2006], in situ observations from deep sea ocean bottom pressure sensors [*Rietbroek et al.*, 2006; *Park et al.*, 2008] as well as sterically corrected satellite altimetry and predictions from ocean general circulation models [*Dobslaw and Thomas*, 2007]. By utilizing the relation between bottom pressure gradients and ACC transport variations, *Zlotnicki et al.* [2007] derived seasonal variations in ACC transport variability from early GRACE data sets, and compared them to predictions from numerical ocean models. While *Böning et al.* [2010] confirmed their general conclusions based on reprocessed GRACE data, their results were as well restricted to a temporal resolution of 30 days.

[6] Besides improvements in the overall accuracy of the GRACE gravity fields, progress has been also made in achieving a higher temporal resolution. In this paper, two alternative GRACE products with daily and 10 day sampling will be therefore tested for their ability to accurately represent ocean bottom pressure gradients and therefore transport in the Southern Ocean. Data sets and necessarily applied postprocessing procedures are described in section 2. Bottom pressure variability as seen by these GRACE products is validated with respect to in situ bottom pressure observations. Analysis is separated into three different intraseasonal frequency bands in order to allow an intercomparison of these differently sampled GRACE time series (section 3). The relationof bottom pressure gradients in the southern Pacific with transport variations in Drake Passage and sea level variability around Antarctica is demonstrated by means of an ocean model simulation (section 4) in order to discuss the suitability of those variables to predict ACC transports on different time scales. Transport variations as derived from different GRACE products are subsequently evaluated by means of sea level variability from coastal tide gauge observations around Antarctica (section 5) and anindex for the Southern Annular Mode (section 6), followed by some concluding remarks in the final section.

2. Estimating Ocean Bottom Pressure Variations From GRACE Gravity Fields

[7] The twin-satellite mission GRACE has been specifically designed to map spatiotemporal variations of the Earth's gravity field. The mission aims at a nominal accuracy of $\sim$1 cm geoid height on regional scales of around 500 km and a temporal resolution of one month [*Tapley et al.*, 2004]. Primary observables are highly accurate distances and relative velocities between the two spacecrafts obtained from a microwave ranging system, accompanied by accelerometer data to separate nongravitational forces, as well as GPS and star camera observations for position and attitude control of the satellites.

[8] The standard methodology of the main processing institutions Center for Space Research at the University of Texas (CSR), Jet Propulsion Laboratory (JPL) and Deutsches GeoForschungsZentrum (GFZ) uses data for a period of about 30 days to determine monthly solutions. To reduce nontidal variations in atmosphere and ocean, the AOD1B RL04 products [*Flechtner*, 2007] are applied. These background models consist of atmospheric mass anomalies from the ECMWF operational data and mass anomalies from the global ocean circulation model OMCT [*Thomas et al.*, 2001], driven by corresponding ECMWF atmospheric fields. Stokes coefficients [*Wahr et al.*, 1998] are provided up to spherical harmonic degree/order (d/o) 120. In this paper, we use monthly gravity field solutions of the latest release 04 from GFZ [*Schmidt et al.*, 2008] covering the time period of February 2003 to August 2009.

[9] Other scientific institutions use different processing strategies to calculate global gravity fields with higher temporal resolution. CNES/GRGS (Centre National d'Etudes Spatiales/Groupe de Recherches de Géodésie Spatiale) determines 10 day gravity field solutions up to d/o 50 [*Bruinsma et al.*, 2010]. CNES/GRGS solves stacked 10 day normal equations with additional constraints based on the formal covariances of the coefficients. Due to a degree- and order-dependent stabilization matrix, each coefficient's noise is reduced individually between d/o 16–36 which leads to a greater signal contribution in the higher degrees. Instead of OMCT, the barotropic MOG2D ocean model [*Carrère and Lyard*, 2003] is applied at CNES/GRGS to reduce nontidal ocean variability. Seven years of 10 day gravity field solutions of the most recent release 02 for a time period of August 2002 to August 2009 are used in our study.

[10] Improving the temporal resolution by reducing the time span of observations that enter into a single solution necessarily decreases the spatial resolution, since a smaller number of gravity field parameters can be solved for in a least squares adjustment process. To overcome this problem, the University of Bonn introduced a new approach to estimate daily gravity field solutions, ITG-GRACE2010 (Institute for Theoretical Geodesy), by means of a Kalman Smoother [*Kurtenbach et al.*, 2009]. Assuming that the gravity field parameters of the current day are correlated to (and thus predictable from) the previous ones, a first-order Markov process can be described. Empirical signal covariances characterizing the expected changes of the fields have been derived from multiyear time series of geophysical models describing variability in atmosphere, ocean and continental hydrosphere. AOD1B RL04 has been applied to reduce the short-term nontidal variations of the gravity field as well [*Kurtenbach*, 2011]. The daily gravity field solutions are estimated up to d/o 40.

[11] Changes in ocean bottom pressure represent the summarized effect of mass changes within the above-lying ocean and atmosphere. Since these signals have been at best fully removed during processing by applying the dealiasing product as background model, its time averaged field (i.e., the GAC product for the combined effect of atmosphere and ocean in GRACE terminology) must be added back to restore the signal. Additionally, degree 1 terms, which represent variations of the center of mass with respect to a terrestrial reference frame, are required from auxiliary sources. A mean annual sinusoid determined from Satellite Laser Ranging and DORIS observations [*Eanes*, 2000] has been applied here.

[12] Since we are interested in changes of oceanic mass, spectral leakage of continental signals is minimized following *Wahr et al.* [1998]. In addition, meridional striations occur in the solutions due to inherent properties of the GRACE observation geometry. These effects can be reduced by d/o-dependent spatial filtering of the Stokes coefficients with a nonisotropic two-point kernel function [*Kusche*, 2007], which works in the same way as a Tikhonov-type regularization of the normal equation system. By taking an approximation of the error covariance matrix from GRACE and an a priori signal covariance matrix into account, the north-south correlations of the field are removed. This anisotropic decorrelation filter was only applied to the monthly GFZ gravity field solutions. Due to additional constraints applied during processing of both the CNES/GRGS (regularization) and the ITG-GRACE2010 solutions (Kalman smoother), an additional filtering of these products is not appropriate.

[13] Stokes coefficients ΔC_{lm}, ΔS_{lm} from GRACE for a given time epoch t are finally transformed into bottom pressure anomalies according to *Wahr et al.* [1998]:

$$\Delta p_{bot}(\phi,\lambda,t) = \frac{a_E g \rho_E}{3} \sum_{l=1}^{N} \sum_{m=0}^{l} \frac{2l+1}{1+k_l} P_{lm}(\sin\phi) \times \{\Delta C_{lm}\cos m\lambda + \Delta S_{lm}\sin m\lambda\}, \quad (1)$$

with a_E the semi major axis; ρ_E the Earth's mean density; g the mean gravitational acceleration; k_l are the Love numbers of degree l; P_{lm} the normalized associated Legendre functions of degree l and order m; ϕ is the geographical latitude; and λ the geographical longitude.

3. In Situ Ocean Bottom Pressure

[14] In order to validate bottom pressure variability as seen by GRACE, we use in situ observations from a number of ocean bottom pressure (OBP) recorders. Globally distributed data sets obtained by various institutions were made available by *Macrander et al.* [2010]. The provided data are quality controlled (i.e., elimination of outliers), instrumental drift was removed by a quadratic fit, and tides have been separated by means of the FES2004 tide model [*Lyard et al.*, 2006]. Time series from 21 stations in the Southern Ocean are used in this study (Figure 1). Regional bottom pressure averages from GRACE comparable to these time series have been obtained by applying a pattern filter [*Böning et al.*, 2008]. For this, correlations between ocean bottom pressure anomalies in a maximum radius of 20° have been estimated with model time series from OMCT. Afterward, GRACE data have been filtered by weighting points within the 20° circle with their correlations higher than 0.7 and an additional cut-off function starting at a distance of 18°.

[15] To analyze signals in different frequency bands, filtering of in situ and GRACE bottom pressure time series is required. While smaller gaps have been interpolated for the filtering and flagged as missing values again afterward, gaps of more than 30 days effectively split the record into subsamples that have been treated individually in terms of estimating and removing trends as well as annual and semiannual components. While the GFZ RL04 time series with its monthly sampling was not filtered further, all daily time series have been filtered with a Butterworth filter of order 3, with cut-off periods of 10 and 30 days. Signals are therefore separated into three different frequency bands: (a) periods longer than 30 days (30 days low-pass filter), (b) periods between 10 and 30 days (10 to 30 days band pass filter), and (c) shorter than 10 days (10 days high-pass filter). The 10 day CNES/GRGS RL02 solutions have only been filtered with the 30 days low-pass filter and afterward separated into the first two frequency bands. All subsequent analyses in this paper will refer to a separation of the signals into these three frequency bands.

[16] For periods above 30 days, correlations are generally strong for all GRACE solutions considered (Figure 2). Coherence is particularly high in the South Atlantic and Indian Ocean, where correlations of up to 0.8 and explained variances of 3 hPa^2 are obtained for GFZ. Correlations with bottom pressure records from the Crozet-Kerguelen region in the Indian Ocean are on the order of 0.7, in line with previous findings in the region based on early GRACE releases [*Rietbroek et al.*, 2006]. Correspondence is substantially smaller for stations in the Southern Pacific, with significant correlations obtained only for the ITG-GRACE2010 data, while GFZ and CNES/GRGS show insignificant correlations and zero or even negative explained variances here. However, in situ time series available from the area are rather short and mostly located in subtropical latitudes, where bottom pressure variability is expected to be weak and thus more difficult to observe by GRACE. Note that statistics based on monthly mean averages instead of low-pass-filtered series do not reveal significant differences in correlations and explained variances.

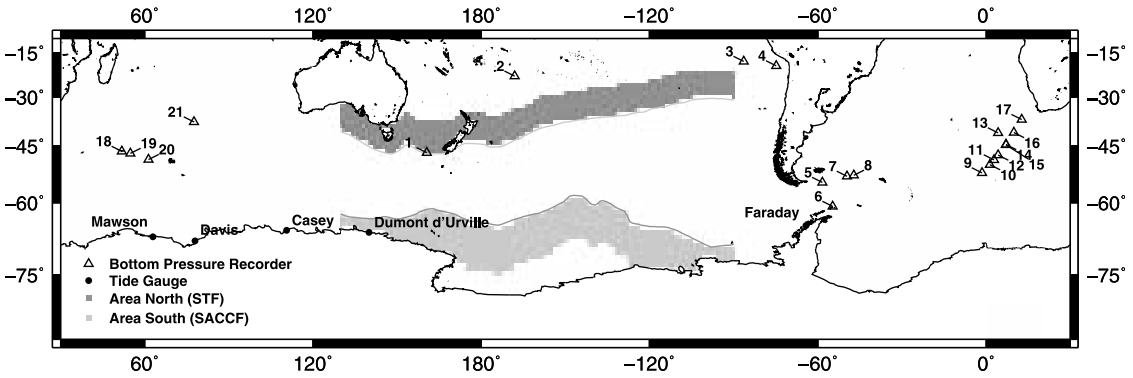

OBP station names		
△ 1 – DART 55015	△ 8 – POL SHAGEX1	△ 15 – AWI ANT7–2
△ 2 – DART 51426	△ 9 – AWI ANT13a	△ 16 – AWI ANT5
△ 3 – DART 32412	△ 10 – AWI ANT11	△ 17 – AWI ANT3
△ 4 – DART 32401	△ 11 – AWI ANT10	△ 18 – CNES CRO
△ 5 – POL ND2	△ 12 – AWI ANT9	△ 19 – POL IO1
△ 6 – POL SD2	△ 13 – AWI ANT537	△ 20 – POL IO2
△ 7 – POL SHAGEX2	△ 14 – AWI ANT7–1	△ 21 – CNES AMS

Figure 1. Location of in situ records available for this study: time series of sea level variations from coastal tide gauges in Antarctica (solid dots) and time series from offshore bottom pressure recorders in the Southern Ocean (triangles). Shaded areas indicate averaging areas for GRACE bottom pressure differences following the path of the Subtropical Front (STF) in the north (dark grey) and the Southern ACC Front (SACCF) in the south (light grey) given by *Orsi et al.* [2001].

[17] Band pass–filtered signals with periods between 10 and 30 days generally correlate better with ITG-GRACE2010 than CNES/GRGS. Explained variances frequently approach 2 hPa^2 for ITG-GRACE2010 in the South Atlantic, while the French solution typically remains below 1 hPa^2. Results are in particular promising in the South Atlantic region, where several multiyear in situ time series collected by the Alfred Wegener Institute (AWI) are available.

[18] Variability beyond 10 days is solely accessible from the ITG-GRACE2010 solutions. High correlations together with generally positive explained variances suggest that ITG-GRACE2010 does contain information on high-frequency ocean dynamics. Power spectra of bottom pressure from ITG-GRACE2010 and in situ observations (not shown) are comparable for both data sets in that band. It can be inferred that modes between 9 and 7 days dominate most stations in the Southern Ocean. This is consistent with the results of *Weijer and Gille* [2005], who found modes with such frequencies in the transport from a constant density, multilevel model of the Southern Ocean. In particular, a mode with a period of 8.3 days is apparent in the bottom pressure data. This topographically trapped mode is excited by the local bathymetry in the area of the East Pacific Rise south west of Africa. Due to the fact that the flow of the ACC goes through this region, the mode affects the ACC directly and therefore leads to a change in meridional ocean bottom pressure, which can be tracked by the OBP stations near the current.

[19] In addition to the different GRACE solutions, simulated bottom pressure variations from OMCT are included into Figure 2. OMCT is routinely applied as a background model to remove nontidal ocean variability in the GRACE processing and can be thus assumed to represent the a priori knowledge already available without flying a satellite gravity mission. Therefore, results from the various GRACE releases assessed in this paper are expected to provide additional information that goes beyond the predictions of OMCT. Here, results from OMCT simulations included in the release 04 of GRACE dealiasing product [*Flechtner*, 2007] are shown. Apart from the stations in the South Atlantic, the different GRACE releases are generally able to explain more of the variability contained in the in situ observations than the model. This is particularly true for the high-frequency band, indicating the ITG-GRACE2010 indeed provides information on nontidal mass variability on synoptic time scales that have not been introduced by the applied background model but originate instead from the processing approach developed at the University of Bonn.

4. Bottom Pressure Gradients, Sea Level Variations, and Transports Through Drake Passage From OMCT

[20] Following the theoretical arguments of *Hughes et al.* [1999], we assume that (a) bottom pressure gradients averaged over the circumpolar flow path of the ACC are representative for its transport across Drake Passage, and (b) sea level variability along the Antarctic coast might serve as a proxy for the bottom pressure gradient. We reassess those relationships on subseasonal time scales focused on in this paper by means of model data from OMCT.

[21] The zonal geostrophic component of the anomalous transport is obtained from the meridional bottom pressure gradient [*Hughes et al.*, 1999]

$$T_g = \frac{H}{f\rho_0}(p_b - p_a), \tag{2}$$

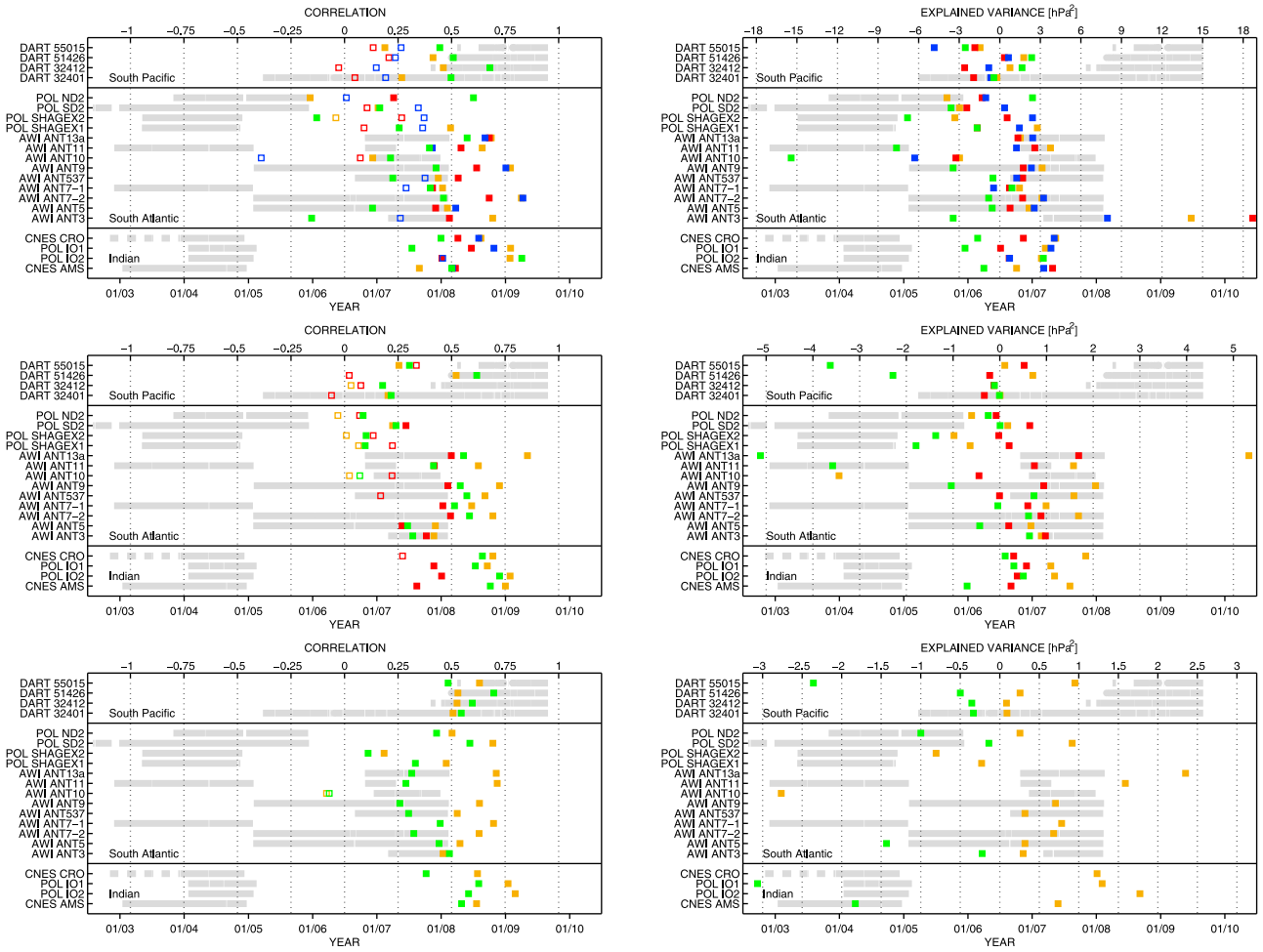

Figure 2. (left) Correlations and (right) explained variances of ocean bottom pressure from ITG-GRACE2010 (yellow), CNES/GRGS (red), and GFZ (blue) and as simulated with OMCT (green) with all available time series from offshore bottom pressure recorders in the Southern Ocean. Filled squares indicate significant correlation at a confidence interval of 95%; open squares are found not significant. Signals have been separated into three different frequency bands containing signals with (top) periods longer than 30 days, (bottom) periods shorter than 10 days, and (middle) band pass–filtered variability between 10 and 30 days. The grey bars indicate the time span of bottom pressure recordings available.

where H is the mean water depth; f the Coriolis parameter; $\rho_0 = 1030.93$ kg/m^3 a mean density of seawater; and p_a, p_b the pressure anomaly at the southern and northern rim of the current, respectively. Bottom pressure and sea surface height fields as well as total transports across Drake Passage at daily resolution have again been obtained from the OMCT simulation that was utilized for the AOD1B RL04 dealiasing product.

4.1. ACC Fronts in the Southern Pacific

[22] The meridional extent of the ACC is usually defined to be bounded by the Subtropical Front (STF) in the north, that separates warm, salty subtropical waters from the fresher and cooler subpolar waters, and the Southern ACC Front, in the south, that is indicated by the first appearance of upwelling abyssal waters. In the South Pacific the current is located between 15° and 70° South. In order to describe the ACC transport variability by means of bottom pressure changes, *Hughes et al.* [1999] argues that ocean bottom pressure south to the main ACC flow path is useful proxy of transport variations. In contrast, *Zlotnicki et al.* [2007] suggested that bottom pressure differences between the Subtropical Front (STF) and the Southern ACC Front (SACCF) should be a better representative for the transport variability, in particular when satellite gravity observations are be considered.

[23] To assess the sensitivity of ocean bottom pressure in the Southern Ocean to simulated baroclinic transport in OMCT at Drake Passage, correlation and regression maps between simulated transport and local bottom pressure variability are computed. Positive correlation and regression coefficients are found in lower latitudes (north of −20°), ranging from 0.2 to 0.4 and 1.0 to 3.5 Sv/hPa, where however, the simulated OBP signal is rather weak. At the same time, negative correlations and regression coefficients are obtained south of −60° from −0.2 to −0.7 and −1.0 to −3.0 Sv/hPa close to the Antarctic coast (see Figure 3).

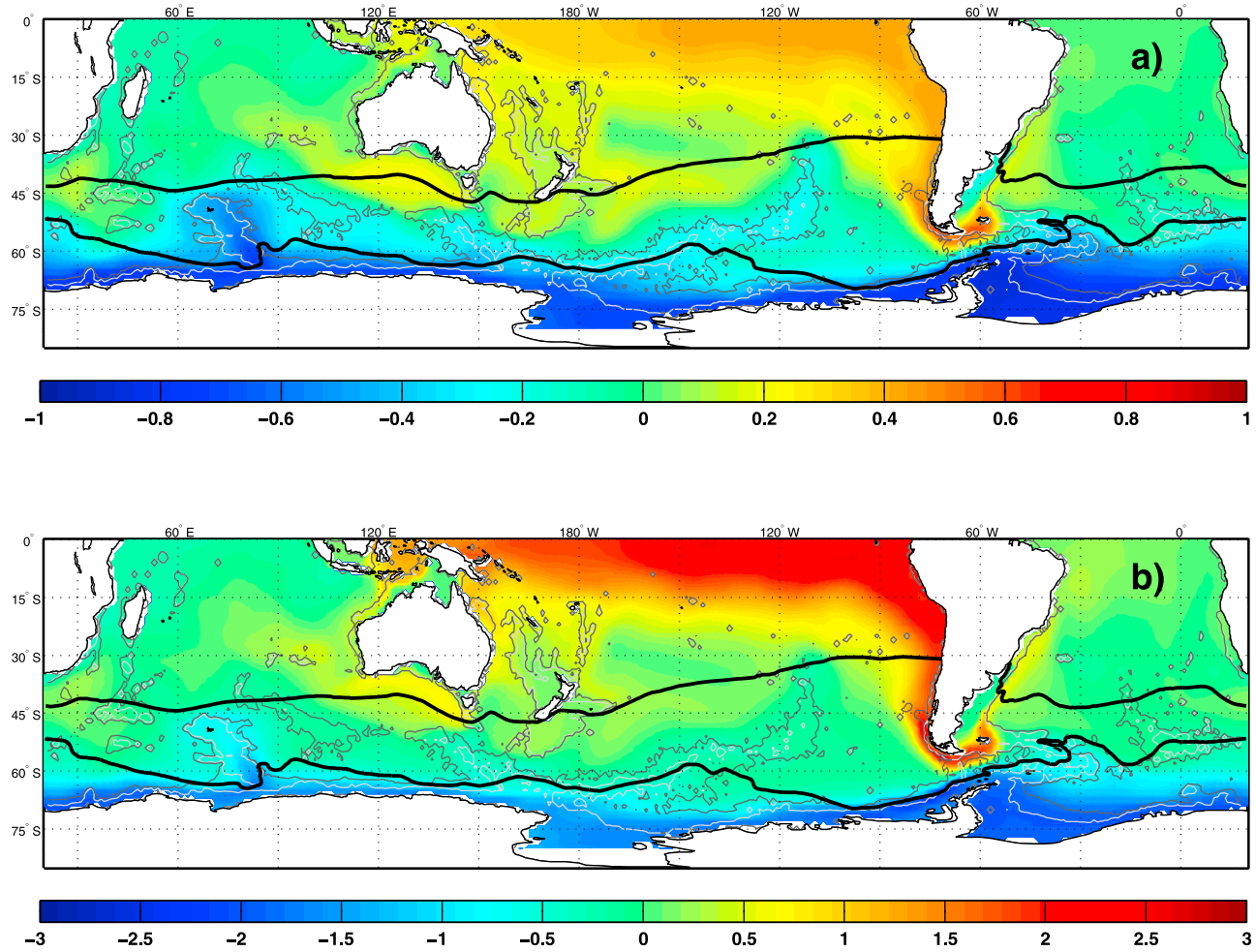

Figure 3. (a) Correlation and (b) regression in Sv/hPa of ocean bottom pressure and transport variations in Drake Passage from OMCT; path of the Subtropical Front (STF, upper black line) and Southern ACC Front (SACCF, lower black line); contours show *f*/*H* quotients, corresponding to depths of 3000 m (light grey) and 4000 m (dark grey).

[24] Comparing those model results with various estimates of the different ACC fronts [*Orsi et al.*, 1995; *Sallée et al.*, 2008; *Sokolov and Rintoul*, 2009], we choose to select 500 km wide averaging regions north of the STF and south of the SACCF, which essentially follow the suggestions by *Zlotnicki et al.* [2007]. Positions of the those fronts have been obtained from *Orsi et al.* [2001].

4.2. Sea Level Variations From OMCT

[25] Sea surface height fields from OMCT are corrected for the effect of atmospheric loading by assuming an ideal inverse barometer [*Wunsch and Stammer*, 1997]. From those fields, two time series have been derived: (1) mean sea level variability around Antarctica, by averaging all coastal cells as defined by the OMCT bathymetry, and (2) sea level variability at the position of the Faraday tide gauge at the Antarctic Peninsula. This position has been selected since at Faraday base (operated since 1996 by Ukraine under the name Vernadsky) a multiyear record of high-quality sea level observations exists that has been previously shown to be an ideal proxy data set for ACC transport variability [e.g., *Hughes et al.*, 2003].

4.3. Analysis of Simulated Time Series From OMCT

[26] From all OMCT data sets, i.e., the full transports through Drake Passage (multiyear mean transport for January 2002 through December 2009 is 118 $\pm$ 9 Sv), bottom pressure and sea level time series, we estimate and remove linear trends as well as annual and semiannual sinusoids (Figure 4). The anomalies are subsequently separated into three different frequency bands as defined above. We calculate bottom pressure gradients from two paths defined by the STF and SACCF (hereafter referred to as bottom pressure gradients) and bottom pressure from the region south of the SACCF (hereafter referred to as the SACCF region bottom pressure), both averaged over the width of the South Pacific as indicated in Figure 1.

[27] Highest correlations for the low-pass-filtered time series are obtained between Drake Passage transports and the mean sea level variability all around Antarctica (-0.94, see Table 1). Correlation with sea level at Faraday is only slightly weaker (-0.88), supporting the notion that the station is indeed well placed to monitor transport variability at Drake Passage. Geostrophic contributions to the flow

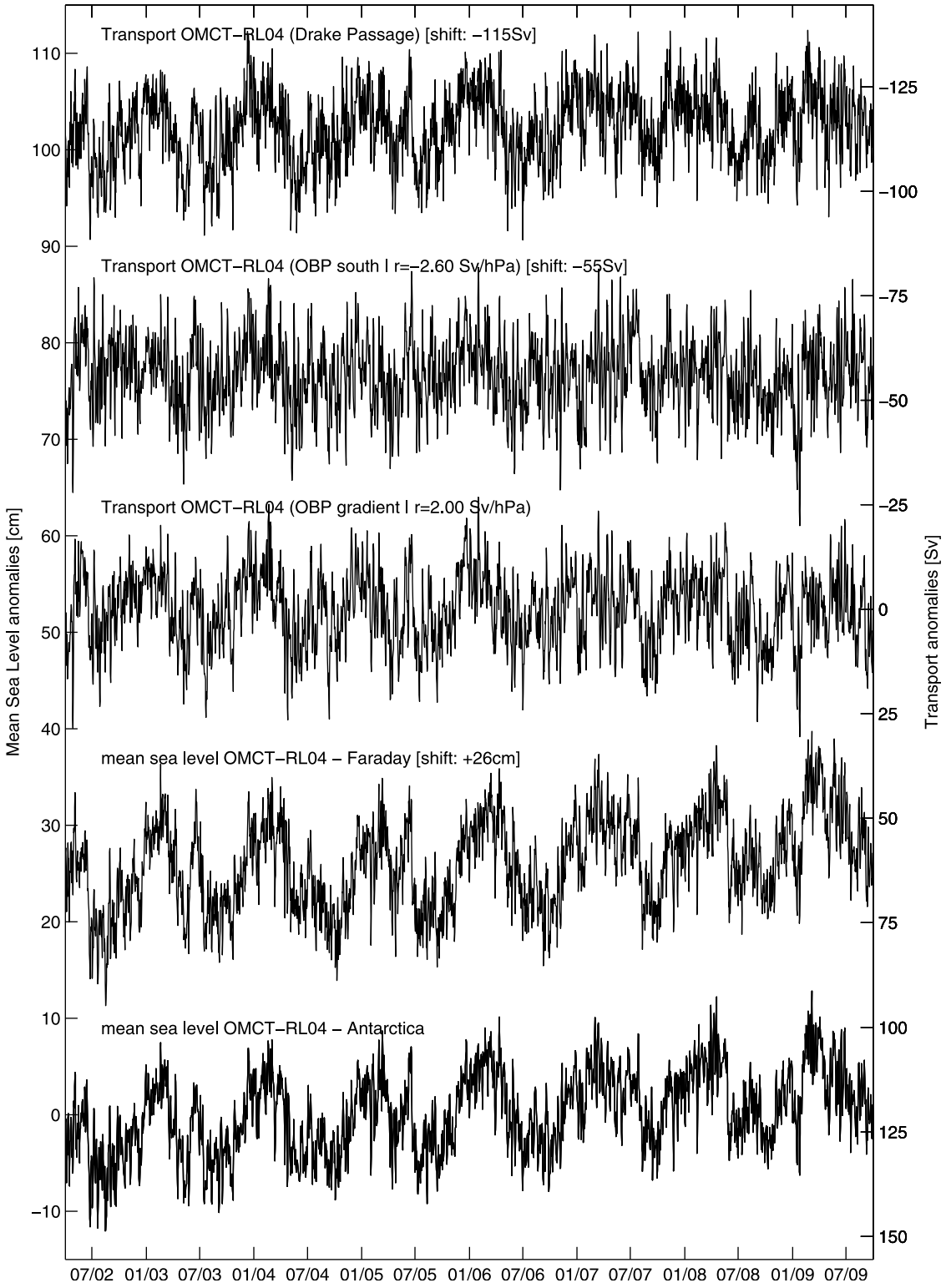

Figure 4. Simulated OMCT time series (unfiltered daily resolution) of the full ACC transport across Drake Passage, the geostrophic component of the transport as derived from bottom pressure gradients (STF-SACCF), and bottom pressure variations south of the SACCF across the Pacific, as well as sea level variations averaged along the coast of Antarctica and at the position of Faraday gauge. Note that transports refer to scale on the right, which has been inverted for ease of comparison.

Table 1. Correlations Between Time Series Simulated by OMCT[a]

	Transport (DP)	SAM	MSL Antarctica	OBP Antarctica	MSL Faraday
30 days low-pass filter					
STF-SACCF	0.79	0.62	−0.84	−0.83	−0.77
SACCF	−0.86	−0.67	0.88	0.87	0.79
Transport (DP)		0.61	−0.94	−0.94	−0.88
MSL Antarctica					0.94
10–30 days band pass filter					
STF-SACCF	0.55	0.56	−0.62	−0.59	−0.57
SACCF	−0.60	−0.53	0.61	0.61	0.54
Transport (DP)		0.41	−0.84	−0.85	−0.78
MSL Antarctica					0.95
10 days high-pass filter					
STF-SACCF	0.29	0.41	−0.65	−0.65	−0.47
SACCF	−0.19	−0.37	0.57	0.59	0.37
Transport (DP)		0.17	−0.51	−0.51	−0.50
MSL Antarctica					0.81

[a]Index for the Southern Annular Mode (SAM), full ACC transport across Drake Passage (DP), geostrophic component of the ACC transport as derived from bottom pressure gradients from Subtropical Front and Southern ACC Front defined by *Orsi et al.* [1995], mean sea level (MSL) and ocean bottom pressure (OBP) averaged along the coastline of Antarctica, and mean sea level at the position of Faraday tide gauge.

obtained from bottom pressure gradients and SACCF region bottom pressure are correlated with Drake Passage transport with 0.79 and −0.86, indicating that a large part of the flow can be tracked by both pressure gradients as well as by bottom pressure variations in the SACCF region. When the coastal bottom pressure variability all along the Antarctic coastline is considered, correlations are not significantly different, i.e., −0.83 with bottom pressure gradients. This results partly from the hydrostatic approximation in OMCT modeling, inducing a linear connection between sea level and ocean bottom pressure variations, and the limited spatial resolution of OMCT. At 1.875° spatial resolution, the model does not reproduce mesoscale eddies, suggesting that the correspondence between sea level and bottom pressure is certainly exaggerated in OMCT.

[28] For higher frequencies, correlations between transport and both bottom pressure gradients and SACCF region bottom pressure are still significant at the 95% confidence level, indicating that transport variability can be indeed explained by ocean bottom pressure observations even on time scales of a few days. However, bottom pressure gradients show slightly higher correlations with both Drake Passage transport and sea level variations when compared to SACCF region bottom pressure, indicating that bottom pressure gradients averaged over the South Pacific might be more appropriate to monitor the flow variability at shorter periods.

[29] In addition, potential error sources in the GRACE estimates, which include leakage of terrestrial water storage and ice mass variations into the ocean domain, remaining systematic errors that are primarily correlated in meridional direction, as well as less well constrained low-degree Stokes coefficients, are expected to affect more strongly estimates of SACCF region bottom pressure close to the Antarctic coast than bottom pressure gradients. In the remainder of this study, we therefore primarily rely on GRACE results obtained from bottom pressure gradients between STF and SACCF, while SACCF region estimates are only occasionally included for comparison.

4.4. Estimation of Optimal Regression Factor Between Ocean Bottom Pressure and Transport Variations

[30] For equation (2) to be valid, the current is required to flow along H/f contours that encircle the Antarctic continent. This path of the current is assumed to be constant in time. Transport and pressure gradient simulated with an ocean model can therefore be used to estimate an effective value for H/f [*Hughes et al.*, 1999]. Using OMCT model time series from transport variations in Drake Passage that were filtered with a 30 days low-pass filter, a regression coefficient of 1.4 Sv/hPa for bottom pressure gradients between STF and SACCF, and −2.1 Sv/hPa for ocean bottom pressure variations south of the SACCF is estimated. These regression factors explain the model transport variance with ocean bottom pressure gradient to 62% and with SACCF region bottom pressure to 73%.

[31] Those regression values are lower than in previous studies. *Meredith et al.* [1996] obtained values of 2.70 Sv/hPa and 2.26 Sv/hPa between two bottom pressure gauges situated north and south of the main current by assuming the transport variability is entirely barotropic. Similar arguments were applied by *Zlotnicki et al.* [2007], who derived a value of 3.1 Sv/hPa for the pressure gradient across the current with an average depth H and geographical latitude ϕ. Although up to 3.7 Sv/hPa were obtained for subsurface pressure along the coast of Antarctica based on FRAM model simulations [*Hughes et al.*, 1999]. More recent analyses of OCCAM model output indicated a relation of only 1.2 Sv/hPa with bottom pressure observations at station SD2 south of Drake Passage [*Hughes et al.*, 2003], suggesting that assuming entirely barotropic conditions is certainly not justified by observations. These lower regression coefficients are also supported by *Whitworth and Peterson* [1985], who used in situ data of transport moorings and bottom pressure recorders at each side of Drake Passage to obtain a regression value of 1.9 Sv/hPa.

[32] In order to justify our scaling coefficient more tightly, additional simulations with a new OMCT model version at 1° resolution have been evaluated. From this simulation, we get regression values of 2.2 Sv/hPa and −3.1 Sv/hPa for pressure gradients and SACCF region bottom pressure, respectively. In view of the apparent dependence from the model configuration employed, we decide to rely on approximate values of 2.0 Sv/hPa and −2.6 Sv/hPa to subsequently translate bottom pressure gradients and SACCF

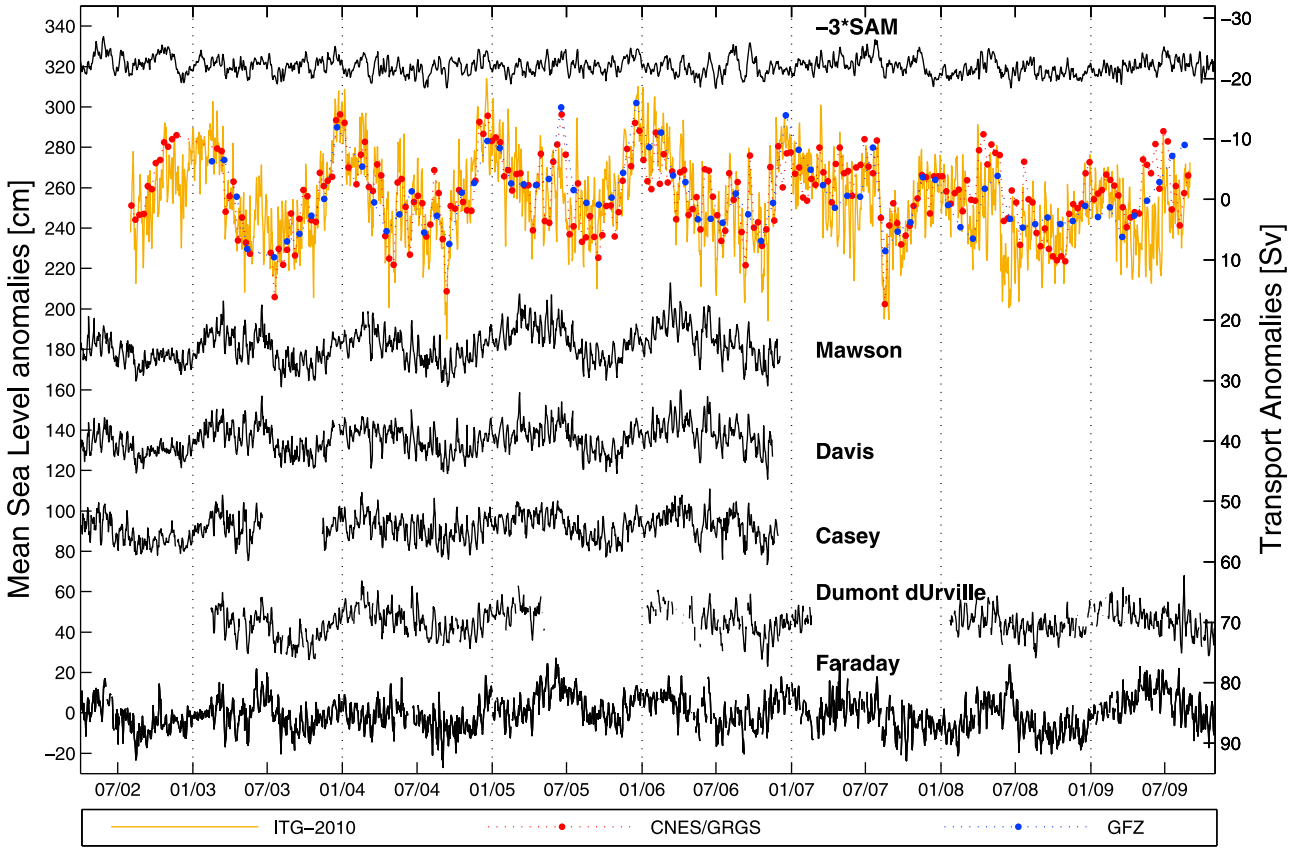

Figure 5. Geostrophic ACC transport anomalies (unfiltered, up to daily resolution) as derived from different GRACE products with regression factor r = 2.0 Sv/hPa, time series of sea level variations at different coastal tide gauges. Geostrophic daily values of SAM index (normalized values multiplied with factor −3 on left axis); transport estimated from different GRACE solutions, and (IB-corrected) sea level at Mawson, Davis, Casey, Dumont d'Urville, and Faraday.

region bottom pressure from GRACE into ACC transport variations in the next section.

5. ACC Transports From GRACE and Antarctic Sea Level Observations

[33] Following equation (2), ACC transports are derived from the three different GRACE bottom pressure distributions from GFZ, CNES/GRGS and ITG-GRACE2010 by averaging over the bottom pressure gradients indicated in Figure 1, and contrasted against tide gauge observations from the Antarctic continent. Hourly tide gauge data covering the study period were available at four stations in the Australian Sector (Casey, Mawson, Davis and Dumont d'Urville) as well as at Faraday on the Antarctic Peninsula (T. Schöne, personal communication, 2011). Hourly tide gauge data have been transformed to daily values by applying a Doodson filter in order to damp out the main tidal frequencies [*Intergovernmental Oceanographic Commission*, 1985]. Subsequently, daily atmospheric data from ECMWF were used to correct the sea level series for inverse barometric effects. As for the transports, a long-term mean, trend, as well as annual and semiannual periodic terms have been removed from the sea level anomalies prior to comparison.

[34] Transport anomalies derived from the three different GRACE solutions are broadly consistent with each other (Figure 5). RMS variabilities for 30 day low-pass-filtered solutions are 3.6 Sv for GFZ, 3.3 Sv for CNES/GRGS and 2.8 Sv for ITG-GRACE2010. ITG-GRACE2010 daily solution exhibits substantial high-frequency variability which cannot be reflected by the other two series, but which is also apparent in the tide gauge data. While concentrating on signal periods longer than 30 days, highest correlations of more than 0.6 are obtained between GFZ- and CNES/GRGS-based transports and sea level variations at Mawson (Table 2). Correlations are approximately two tenths lower with respect to the synthetic OMCT data, indicating both the impact of observation errors and the contribution of mesoscale near-surface variability as discussed above.

[35] For variability between 10 and 30 days, correlations drop to around 0.3 for most tide gauges, while CNES/GRGS and ITG-GRACE2010 are still showing good agreement to each other. For the high-frequency variability with periods below 10 days, correlations forITG-GRACE2010 vary for all tide gauges between −0.15 and −0.27 which is consistent with the value of 0.2 as found from OMCT model data, underlining the weak but significant connection between geostrophic transport variabilities and sea level variations even on the shortest time scales considered.

[36] Linear regression coefficients of transport variations estimated from GFZ RL04, CNES/GRGS and ITG-GRACE2010 solutions and 30 day low-pass-filtered mean

Table 2. Correlation Between Observed Time Series[a]

	SAM	ITG-GRACE2010	CNES/GRGS	GFZ
Periods longer than 30 days				
Faraday	−0.44	−0.46 (0.47)	−0.39 (0.37)	−0.56 (0.58)
Dumont d'Urville	−0.56	−0.52 (0.54)	−0.45 (0.47)	−0.45 (0.47)
Casey	−0.64	−0.55 (0.50)	−0.59 (0.55)	−0.52 (0.53)
Davis	−0.49	−0.46 (0.39)	−0.52 (0.54)	−0.50 (0.55)
Mawson	−0.63	−0.51 (0.45)	−0.61 (0.60)	−0.58 (0.61)
SAM		0.67 (−0.58)	0.72 (−0.70)	0.63 (−0.60)
Periods between 10 and 30 days				
Faraday	−0.38	−0.27 (0.18)	−0.15 (0.13)	
Dumont d'Urville	−0.43	−0.33 (0.29)	−0.34 (0.35)	
Casey	−0.38	−0.31 (0.24)	−0.33 (0.32)	
Davis	−0.35	−0.30 (0.21)	−0.28 (0.31)	
Mawson	−0.39	−0.30 (0.22)	−0.26 (0.29)	
SAM		0.52 (0.26)	0.46 (−0.39)	
Periods shorter than 10 days				
Faraday	−0.16	−0.22 (0.19)		
Dumont d'Urville	−0.36	−0.23 (0.22)		
Casey	−0.26	−0.27 (0.23)		
Davis	−0.30	−0.19 (0.16)		
Mawson	−0.28	−0.17 (0.14)		
SAM		0.32 (0.15)		

[a]Mean sea level at various tide gauges all along the coast of Antarctica (Faraday, Dumont d'Urville, Casey, Davis, Mawson), geostrophic transport derived from ocean bottom pressure gradients (ocean bottom pressure variations of southern path) across the Pacific as seen by different GRACE products (ITG-GRACE010, CNES/GRGS, GFZ), and an index for the Southern Annular Mode (SAM).

sea level data from tide gauges vary between −0.43 to −0.51 Sv/cm, −0.33 to −0.63 Sv/cm and −0.35 to −0.58 Sv/cm each. Even in the low-pass-filtered band the time series of tide gauge stations show more variability than estimated transport variations from GRACE, which might be related to local effects affecting the tide gauges (e.g., sea ice, fresh water fluxes from the continent) which are not sensed by a satellite gravity mission.

6. ACC Transports From Model and GRACE and the Southern Annular Mode

[37] There is strong evidence in terms of both observations and theoretical reasoning (see *Meredith et al.* [2004] for a summary) that a strong relation exists between ACC transport variability and the prevailing surface wind field in middle latitudes of the Southern Hemisphere. By means of the ECCO model and monthly GRACE solutions, *Ponte and Quinn* [2009] demonstrated a connection between ocean bottom pressure variations and zonal wind stress anomalies which is induced by Ekman dynamics in the Southern Ocean. ACC transports from OMCT and GRACE as well as sea level observations are therefore contrasted against an index for the Southern Annular Mode (SAM) provided by the CPC (Climate Prediction Center, available from http://www.cpc.ncep.noaa.gov). This normalized daily index is based on a loading pattern obtained from the leading EOF of geopotential height anomalies at the 700 hPa level in the Southern Hemisphere poleward of 20° over a base period of two decades, multiplied with the daily pressure distribution. As for all time series considered in this study , trend as well as annual and semiannual harmonics are removed. The reduced index is displayed in Figure 5 and has been subsequently separated into the three different frequency bands.

[38] A linear regression of daily OMCT transport variations and the SAM index gives a ratio of 2.6 Sv/[unit SAM]. The time series of the SAM index has a standard deviation of 1.1 [unit SAM]. This result is close to the values estimated by *Hughes et al.* [2003] with modeled transport of OCCAM (2.8 Sv/[unit SAM]). In the 30 day low-pass-filtered domain correlations between SAM and transport in Drake Passage and in the South Pacific lie in the range of 0.61 to 0.62 (−0.67 for SACCF; see Table 1).

[39] Comparing SAM with GRACE results and sea level variations from Antarctic tide gauges for periods longer than 30 days, wind variability is strongly correlated with sea level records from all five available stations, with highest correlations of 0.64 obtained for Casey. In addition, correlations between SAM and the transports from different GRACE products are equally high, approaching 0.72 for the CNES/GRGS solutions. These values are substantially higher than any of the correlations between GRACE and a single tide gauge record, indicating that GRACE indeed sees hemispherically coherent mass variations that are connected to the prevailing winds.

[40] Correlations between SAM and GRACE are substantially weaker for the band pass–filtered signals with periods between 10 and 30 days, with maximum correlations of 0.52 obtained for the ITG-GRACE2010 bottom pressure estimates and 0.32 for periods below 10 days. These correlations are slightly lower than estimates from OMCT model results (0.56 for band pass filter and 0.41 for high-pass filter) and appear plausible since the noise level is generally increasing at higher frequencies (and hence shorter averaging intervals), where transient weather features start to dominate local observations.

[41] Finally, lagged correlations between bottom pressure gradients from ITG-GRACE2010 and SAM in the low-pass-filtered band reveal a time shift of one day. This is in contrast to the results given by *Wearn and Baker* [1980], who found a time lag of nine days when correlating hemispherically wind and transport variations in Drake Passage. Even in the high-pass filtered band the time lag is less than one day. A comparable time lag has been obtained by *Wearn*

and Baker [1980] only for the relation of local wind and subsurface pressure variation in Drake Passage. Initial results obtained here from ITG-GRACE2010 indicate that the adjustment of bottom pressure to changing surface winds is even on a hemispheric scale much faster than thought before.

7. Summary and Conclusions

[42] Newly available gravity field solutions with higher than monthly temporal sampling have been evaluated in terms of their information content on Southern Ocean dynamics. Validation of bottom pressure distributions against a limited number of available in situ records indicates that GRACE is indeed able to provide bottom pressure variability with periods down to a few days, when advanced processing concepts as the Kalman filtering approach developed at the University of Bonn are applied.

[43] Pressure gradients from GRACE across the Pacific translated into geostrophic transport anomalies of the ACC in Drake Passage with applying a regression coefficient of 2.0 Sv/hPa vary in a range of $\pm$20 Sv. They are strongly correlated with sea level variability along the Antarctic coast as inferred from coastal tide gauge data. Correlation is in particularly apparent on time scales longer than 30 days, but significant correlations also exist on periods below 10 days.

[44] In addition, GRACE-based meridional bottom pressure gradients reveal significant (>0.6) correlations with the SAM on periods above 30 days, which is even higher than correlations achieved with any of the tide gauge records. This underlines once more the strong relation of the transport variations (i.e., the bottom pressure distributions they are based on) with the dominant pattern of large-scale atmosphere dynamics on the Southern Hemisphere.

[45] This study indicated that GRACE is able to observe bottom pressure variability that goes beyond the a priori knowledge contained in the background model OMCT. Similar conclusions have been also drawn by *Bonin and Chambers* [2011] from comparisons with satellite-based sea level anomalies. For the upcoming release 05 of GRACE, a new OMCT version with 1° resolution (see section 4.4) is incorporated, that shows substantially improved bottom pressure variability in particular on subweekly periods. In addition to conventionally improved background models, further developments in combining numerical model information with data, either by means of incorporating stochastic a priori information into the gravity field determination process, or by means of incorporating high-resolution geodetic observations into an numerical ocean model by means of data assimilation approaches [*Saynisch and Thomas*, 2012], appear promising to cope with the high-frequency nontidal ocean mass variability sensed by satellite gravity missions.

[46] With new GRACE products available at daily resolution, a combination with more traditional oceanographic observation types can be aspired. This might include the removal of mean barotropic variability from campaign-like current meter observations that are occupied only for a limited time span. Combinations with complementary satellite observations covering identical time frames become also now feasible. While the barotropic flow component is obtained from GRACE, sea surface height anomalies from the satellite altimetry mission TOPEX/Poseidon and its successors can provide information on a large part of the baroclinic variability [*Gille et al.*, 2001]. Improved retracking algorithms suitable to obtain highly accurate sea level anomalies also near the coasts (see, e.g., for recent technological developments, *Gommenginger et al.* [2011]), in connection with an independently obtained high-resolution geoid from GOCE [*Rummel et al.*, 2011] serving as a reference surface for calculating absolute surface geostrophic velocities, calls for a reassessment of previous studies that attempted to monitor the variability of the Antarctic Circumpolar Current from space.

[47] **Acknowledgments.** We thank Tilo Schöne (GFZ) for providing quality-controlled tide gauge data and Andreas Macrander (AWI) for compiling and sharing his OBP database. This work has been supported by Deutsche Forschungsgemeinschaft within the priority program SPP1257 "Mass Transport and Mass Distribution in the System Earth" under grant DO1311/2-1.

References

Bingham, R. J., and C. W. Hughes (2006), Observing seasonal bottom pressure variability in the North Pacific with GRACE, *Geophys. Res. Lett.*, *33*, L08607, doi:10.1029/2005GL025489.

Bonin, J. A., and D. P. Chambers (2011), Evaluation of high-frequency oceanographic signal in GRACE data: Implications for de-aliasing, *Geophys. Res. Lett.*, *38*, L17608, doi:10.1029/2011GL048881.

Böning, C., R. Timmermann, A. Macrander, and J. Schröter (2008), A pattern-filtering method for the determination of ocean bottom pressure anomalies from GRACE solutions, *Geophys. Res. Lett.*, *35*, L18611, doi:10.1029/2008GL034974.

Böning, C., R. Timmermann, S. Danilov, and J. Schröter (2010), Antarctic Circumpolar Current transport variability in GRACE gravity solutions and numerical ocean model simulations, in *System Earth via Geodetic-Geophysical Space Techniques*, *Adv. Tech. Earth Sci.*, vol. 1, edited by F. M. Flechtner et al., pp. 187–199, Springer, Berlin, doi:10.1007/978-3-642-10228-8.

Bruinsma, S., J.-M. Lemoine, R. Biancale, and N. Valès (2010), CNES/GRGS 10-day gravity field models (release 2) and their evaluation, *Adv. Space Res.*, *45*(4), 587–601, doi:10.1016/j.asr.2009.10.012.

Carrère, L., and F. Lyard (2003), Modeling the barotropic response of the global ocean to atmospheric wind and pressure forcing - comparisons with observations, *Geophys. Res. Lett.*, *30*(6), 1275, doi:10.1029/2002GL016473.

Cunningham, S. A., and M. Pavic (2007), Surface geostrophic currents across the Antarctic Circumpolar Current in Drake Passage from 1992 to 2004, *Prog. Oceanogr.*, *73*(3–4), 296–310, doi:10.1016/j.pocean.2006.07.010.

Cunningham, S. A., S. G. Alderson, B. A. King, and M. A. Brandon (2003), Transport and variability of the Antarctic Circumpolar Current in Drake Passage, *J. Geophys. Res.*, *108*(C5), 8084, doi:10.1029/2001JC001147.

Dobslaw, H., and M. Thomas (2007), Simulation and observation of global ocean mass anomalies, *J. Geophys. Res.*, *112*, C05040, doi:10.1029/2006JC004035.

Eanes, R. (2000), SLR solutions from the University of Texas Center for Space Research, Geocenter from TOPEX SLR/DORIS, 1992–2000, http://web.archive.org/web/20071127151309/http:/sbgg.jpl.nasa.gov/datasets.html, IERS Spec. Bur. for Gravity/Geocent., Pasadena, Calif.

Flechtner, F. (2007), GRACE AOD1B product description document for product releases 01 to 04, report, Ger. Res. Cent. for Geosci., Potsdam, Germany.

Gille, S. T., D. P. Stevens, R. T. Tokmakian, and K. J. Heywood (2001), Antarctic Circumpolar Current response to zonally averaged winds, *J. Geophys. Res.*, *106*(C2), 2743–2759, doi:10.1029/1999JC900333.

Gommenginger, C., P. Thibaut, L. Fenoglio-Marc, G. Quartly, X. Deng, J. Gómez-Enri, P. Challenor, and Y. Gao (2011), Retracking altimeter waveforms near the coasts, in *Coastal Altimetry*, edited by S. Vignudelli et al., pp. 61–101, Springer, Berlin.

Hughes, C. W., M. P. Meredith, and K. J. Heywood (1999), Wind-driven transport fluctuations through Drake Passage: A southern mode, *J. Phys. Oceanogr.*, *29*(8), 1971–1992.

Hughes, C. W., P. L. Woodworth, M. P. Meredith, V. Stepanov, T. Whitworth, and A. R. Pyne (2003), Coherence of Antarctic sea levels, Southern Hemisphere Annular Mode, and flow through Drake Passage, *Geophys. Res. Lett.*, *30*(9), 1464, doi:10.1029/2003GL017240.

Intergovernmental Oceanographic Commission (1985), *Manual on Sea Level Measurement and Interpretation: Volume 1—Basic Procedures*, U. N. Educ., Sci. and Cult. Organ., Paris.

Kurtenbach, E. (2011), Entwicklung eines Kalman-Filters zur Bestimmung kurzzeitiger Variationen des Erdschwerefeldes aus Daten der Satellitenmission GRACE, PhD thesis, Univ. of Bonn, Bonn, Germany. [Available at http://nbn-resolving.de/urn:nbn:de:hbz:5 N-25739.]

Kurtenbach, E., T. Mayer-Gürr, and A. Eicker (2009), Deriving daily snapshots of the Earth's gravity field from GRACE L1B data using Kalman filtering, *Geophys. Res. Lett.*, *36*, L17102, doi:10.1029/2009GL039564.

Kusche, J. (2007), Approximate decorrelation and non-isotropic smoothing of time-variable GRACE-type gravity field models, *J. Geodes.*, *81*(11), 733–749, doi:10.1007/s00190-007-0143-3.

Lyard, F., F. Lefevre, T. Letellier, and O. Francis (2006), Modelling the global ocean tides: Modern insights from FES2004, *Ocean Dyn.*, *56*(5–6), 394–415, doi:10.1007/s10236-006-0086-x.

Macrander, A., C. Böning, O. Boebel, and J. Schröter (2010), Validation of GRACE gravity fields by in-situ data of ocean bottom pressure, in *System Earth via Geodetic-Geophysical Space Techniques*, *Adv. Tech. Earth Sci.*, vol. 1, edited by F. M. Flechtner et al., pp. 169–185, Springer, Berlin.

Meredith, M. P., J. M. Vassie, K. J. Heywood, and R. Spencer (1996), On the temporal variability of the transport through Drake Passage, *J. Geophys. Res.*, *101*(C10), 22,485–22,494, doi:10.1029/96JC02003.

Meredith, M. P., P. L. Woodworth, C. W. Hughes, and V. Stepanov (2004), Changes in the ocean transport through Drake Passage during the 1980s and 1990s, forced by changes in the Southern Annular Mode, *Geophys. Res. Lett.*, *31*, L21305, doi:10.1029/2004GL021169.

Olbers, D., and K. Lettmann (2007), Barotropic and baroclinic processes in the transport variability of the Antarctic Circumpolar Current, *Ocean Dyn.*, *57*(6), 559–578, doi:10.1007/s10236-007-0126-1.

Olbers, D., D. Borowski, C. Völker, and J.-O. Wölff (2004), The dynamical balance, transport and circulation of the Antarctic Circumpolar Current, *Antarct. Sci.*, *16*(4), 439–470, doi:10.1017/S0954102004002251.

Orsi, A. H., T. Whitworth III, and W. D. Nowlin Jr. (1995), On the meridional extent and fronts of the Antarctic Circumpolar Current, *Deep Sea Res., Part I*, *42*(5), 641–673, doi:10.1016/0967-0637(95)00021-W.

Orsi, A. H., T. Whitworth III, and W. D. Nowlin Jr. (2001), Locations of the various fronts in the Southern Ocean, http://data.aad.gov.au/aadc/metadata/metadata_redirect.cfm?md=AMD/AU/southern_ocean_fronts, Aust. Antarct. Data Cent., Kingston. [Updated 2008.]

Park, J.-H., D. R. Watts, K. A. Donohue, and S. R. Jayne (2008), A comparison of in situ bottom pressure array measurements with GRACE estimates in the Kuroshio Extension, *Geophys. Res. Lett.*, *35*, L17601, doi:10.1029/2008GL034778.

Ponte, R. M., and K. J. Quinn (2009), Bottom pressure changes around Antarctica and wind-driven meridional flows, *Geophys. Res. Lett.*, *36*, L13604, doi:10.1029/2009GL039060.

Rietbroek, R., P. LeGrand, B. Wouters, J.-M. Lemoine, G. Ramillien, and C. W. Hughes (2006), Comparison of in situ bottom pressure data with GRACE gravimetry in the Crozet-Kerguelen region, *Geophys. Res. Lett.*, *33*, L21601, doi:10.1029/2006GL027452.

Rintoul, S. R., C. Hughes, and D. Olbers (2001), The Antarctic Circumpolar Current system, in *Ocean Circulation and Climate*, *Int. Geophys. Ser.*, vol. 77, edited by G. Siedler, J. Church, and J. Gould, pp. 271–302, Academic, San Diego, Calif.

Rummel, R., M. Horwath, W. Yi, A. Albertella, W. Bosch, and R. Haagmans (2011), GOCE, satellite gravimetry and Antarctic mass transports, *Surv. Geophys.*, *32*, 643–657, doi:10.1007/s10712-011-9115-5.

Sallée, J. B., K. Speer, and R. Morrow (2008), Response of the Antarctic Circumpolar Current to atmospheric variability, *J. Clim.*, *21*(12), 3020–3039, doi:10.1175/2007JCLI1702.1.

Saynisch, J., and M. Thomas (2012), Ensemble Kalman-filtering of Earth rotation observations with a global ocean model, *J. Geodyn.*, doi:10.1016/j.jog.2011.10.003, in press.

Schmidt, R., F. Flechtner, U. Meyer, K.-H. Neumayer, C. Dahle, R. König, and J. Kusche (2008), Hydrological signals observed by the GRACE satellites, *Surv. Geophys.*, *29*, 319–334, doi:10.1007/s10712-008-9033-3.

Sokolov, S., and S. R. Rintoul (2009), Circumpolar structure and distribution of the Antarctic Circumpolar Current fronts: 2. Variability and relationship to sea surface height, *J. Geophys. Res.*, *114*, C11019, doi:10.1029/2008JC005248.

Tapley, B. D., S. Bettadpur, M. Watkins, and C. Reigber (2004), The gravity recovery and climate experiment: Mission overview and early results, *Geophys. Res. Lett.*, *31*, L09607, doi:10.1029/2004GL019920.

Thomas, M., J. Sündermann, and E. Maier-Reimer (2001), Consideration of ocean tides in an OGCM and impacts on subseasonal to decadal polar motion excitation, *Geophys. Res. Lett.*, *28*(12), 2457–2460, doi:10.1029/2000GL012234.

Thompson, D. W. J., and J. M. Wallace (2000), Annular modes in the extratropical circulation. Part I: Month-to-month variability, *J. Clim.*, *13*(5), 1000–1016, doi:10.1175/1520-0442(2000)013<1000:AMITEC>2.0.CO;2.

Wahr, J., M. Molenaar, and F. Bryan (1998), Time variability of the Earth's gravity field: Hydrological and oceanic effects and their possible detection using GRACE, *J. Geophys. Res.*, *103*(B12), 30,205–30,229, doi:10.1029/98JB02844.

Wearn, R. B., Jr., and D. J. Baker Jr. (1980), Bottom pressure measurements across the Antarctic Circumpolar Current and their relation to the wind, *Deep Sea Res., Part A*, *27*(11), 875–888, doi:10.1016/0198-0149(80)90001-1.

Weijer, W., and S. T. Gille (2005), Adjustment of the Southern Ocean to wind forcing on synoptic time scales, *J. Phys. Oceanogr.*, *35*(11), 2076–2089, doi:10.1175/JPO2801.1.

Whitworth, T., III, and R. G. Peterson (1985), Volume transport of the Antarctic Circumpolar Current from bottom pressure measurements, *J. Phys. Oceanogr.*, *15*(6), 810–816.

Woodworth, P. L., et al. (2006), Antarctic Peninsula sea levels: A real-time system for monitoring Drake Passage transport, *Antarct. Sci.*, *18*(3), 429–436, doi:10.1017/S0954102006000472.

Wunsch, C., and D. Stammer (1997), Atmospheric loading and the oceanic "inverted barometer" effect, *Rev. Geophys.*, *35*(1), 79–107, doi:10.1029/96RG03037.

Zlotnicki, V., J. Wahr, I. Fukumori, and Y. T. Song (2007), Antarctic Circumpolar Current transport variability during 2003–05 from GRACE, *J. Phys. Oceanogr.*, *37*(2), 230–244, doi:10.1175/JPO3009.1.